Relativistic strong-field ionization of hydrogenlike atomic systems in constant crossed electromagnetic fields

A. Eckey,[1] M. Klaiber,[2] A. B. Voitkiv,[1] and C. Müller[1]

[1]*Institut für Theoretische Physik I, Heinrich Heine Universität Düsseldorf, Universitätsstraße 1, 40225 Düsseldorf, Germany*

[2]*Lochhofstraße 8, 78120 Furtwangen, Germany*

(Received 13 December 2022; revised 13 February 2023; accepted 21 February 2023; published 20 March 2023)

Relativistic strong-field ionization of hydrogenlike atoms or ions in a constant crossed electromagnetic field is studied. The transition amplitude is formulated within the strong-field approximation in the Göppert-Mayer gauge, with initial and final electron states being described by the corresponding Dirac-Coulomb and Dirac-Volkov wave functions, respectively. Coulomb corrections to the electron motion during tunneling are taken into account by adjusting an established method to the present situation. Total and energy-differential ionization rates are calculated and compared with predictions from other theories in a wide range of atomic numbers and applied field strengths.

DOI: 10.1103/PhysRevA.107.033113

I. INTRODUCTION

The first treatment of strong-field ionization of atoms by an alternating electric field was provided in a seminal work by Keldysh [1], who introduced the strong-field approximation (SFA) in a nonrelativistic context. Shortly after, Nikishov and Ritus [2,3] studied within Klein-Gordon theory the relativistic strong-field ionization of a spinless particle bound by short-range forces in the presence of an electromagnetic plane wave or constant crossed field. Later on, Reiss [4,5] generalized Keldysh's consideration to the relativistic regime by calculating, within Dirac theory, the ionization of a 1s electron bound by Coulomb forces in a plane electromagnetic laser wave. In parallel with the SFA approaches, the Perelomov-Popov-Terentev (PPT) theory of strong-field ionization was developed [6]. It relies on the imaginary-time method and allows for a relativistic generalization of Keldysh's ionization theory as well [7–9]. Reviews on relativistic strong-field ionization are given in [10–12].

Nowadays, it is possible by table-top devices to generate laser pulses with field intensities of the order of 10^{19}–10^{20} W/cm^2 in the optical or near-infrared frequency domain. The motion of a free electron exposed to such intense fields becomes relativistic within less than an oscillation cycle. Experiments on relativistic strong-field ionization of noble-gas atoms have observed the formation of very high charge states with ionization down to the K shell [13–16].

The rich physics of strong-field ionization is correctly described by the SFA in a qualitative manner. In particular, depending on the value of the Keldysh parameter [1], it properly distinguishes the regimes of multiphoton, above-threshold, and tunneling ionization. The method is also capable of describing short laser-pulse effects [17,18]. However, to reach predictive power also in quantitative terms, it needs to be adjusted properly. In standard SFA, the ionized electron is described by the corresponding Volkov state, which takes the interaction with the external electromagnetic (laser) field fully into account but disregards the influence of the atomic core potential on the electron dynamics during tunneling. Accordingly, a correction is needed to incorporate the Coulomb field effects. Corresponding correction factors have been obtained within the framework of the PPT theory [7–9,19–21]. With respect to the SFA, there are heuristic approaches using Coulomb-Volkov wave functions [22]. More recently, it has been shown that the results from the imaginary-time method with Coulomb corrections can be derived from the SFA approach using the eikonal Volkov states for the continuum electron [23–25]. The Coulomb singularity in the phase of the eikonal wave function has been removed, using matching of the continuum wave function to the asymptotics of the undisturbed bound state. More straightforwardly and equivalently, in [26] it has been shown that the explicit calculation of the Coulomb-corrected SFA amplitude for the atomic s states avoids singularities because of the cancellation of the Coulomb divergent contribution from the eikonal phase with a term in the SFA prefactor. Another method for removing the Coulomb singularity in the SFA amplitude has been put forward in the analytical R-matrix theory, via the imaginary-time shifting of the integration in the eikonal phase [27,28]. It is worth mentioning that, apart from the mainly analytical SFA and PPT approaches, also fully numerical studies of the relativistic dynamics and ionization of highly charged ions in very strong laser fields have been carried out [29–36].

Due to the approximations involved, SFA predictions turn out to depend on the gauge that is chosen to describe the external electromagnetic fields. From studies of nonrelativistic strong-field ionization it is known that calculations in the length gauge generally yield better agreement with numerical solutions or experimental data than those in velocity gauge [37]. The relativistic version of the length gauge is the Göppert-Mayer gauge [10,17,26].

In the present paper we provide another treatment of relativistic strong-field ionization of a hydrogenlike atomic

system. As the first step, the earlier approaches in [2–4] are combined to calculate, within Dirac theory and standard SFA, the relativistic ionization of a $1s$ electron bound by a nuclear Coulomb potential in the presence of a constant crossed field (CCF). In contrast to the work by Nikishov and Ritus [2,3], we account for the Coulomb field in the bound state and also for the electron spin. As compared with the work of Reiss [4], we apply a CCF in the Göppert-Mayer gauge rather than an oscillating wave in the radiation gauge. Our study thus forms a link between the seminal papers [2–4]. The choice of the CCF is motivated by the fact that, for small Keldysh parameters, the ionization resembles a tunneling process through the potential barrier that is formed by the field of the atomic core and the laser field [38] which then appears as quasistatic on the timescale of the ionization dynamics.

In the second step we include a suitable Coulomb-correction factor which is obtained by an appropriate modification of the procedure developed in [7–9,19] to the present case. The modification is necessary because the long-range Coulomb potential is already included here in the initial $1s$ bound state of the electron, whereas a short-range binding potential was assumed in the previous studies [7–9,19].

Accordingly, our paper is organized as follows. We present our theoretical approach to relativistic strong-field ionization in Sec. II, starting with the standard SFA calculation in Sec. II A. In Sec. II B we determine an overall Coulomb-correction factor that the SFA rate needs to be multiplied with. An analytical approximation of the Coulomb-corrected ionization rate in closed form is obtained in Sec. II C. We illustrate our approach by numerical results in Sec. III and compare them with predictions from other theories. A summary is given in Sec. IV.

II. THEORETICAL FRAMEWORK

In this section we outline our approach to relativistic ionization in a CCF in the Göppert-Mayer gauge. In the following, we use atomic units (a.u.) throughout, with the elementary charge unit $e = 1$.

A. Ionization rate in standard SFA

The relativistic ionization process in combined laser and Coulomb fields can be described within an S-matrix formalism. The transition amplitude in the SFA can be expressed in the prior form as

$$S^{\mathrm{SFA}} = -\frac{i}{c}\int d^4x\, \bar{\psi}^{(-)}(x)\not{A}_{\mathrm{G}}(x)\Phi_{1s}(x), \tag{1}$$

with the initial state

$$\Phi_{1s}(x) = g(r)\chi_s \exp(-iE_{1s}t) \tag{2}$$

describing the Coulomb-Dirac wave function of the hydrogenlike ground state. It consists of a radial part $g(r) = C_{1s}(2Zr)^{\sigma-1}\exp(-Zr)$, where $C_{1s} = (\frac{Z^3}{\pi}\frac{1+\sigma}{\Gamma(1+2\sigma)})^{1/2}$, the two possible spinors

$$\chi_{+1/2} = \begin{pmatrix} 1 \\ 0 \\ ic\frac{1-\sigma}{Z}\cos\vartheta \\ ic\frac{1-\sigma}{Z}\sin\vartheta\, e^{i\varphi} \end{pmatrix}$$

and

$$\chi_{-1/2} = \begin{pmatrix} 0 \\ 1 \\ ic\frac{1-\sigma}{Z}\sin\vartheta\, e^{-i\varphi} \\ -ic\frac{1-\sigma}{Z}\cos\vartheta \end{pmatrix},$$

and the time evolution. Here $E_{1s} = \sigma c^2$, where $\sigma = [1 - (Z/c)^2]^{1/2}$ indicates the energy of the bound state and Z the nuclear charge number. Correspondingly $I_p = c^2 - E_{1s}$ defines the ionization potential.

The interaction with the CCF in Eq. (1) is given by the four-potential in the Göppert-Mayer gauge

$$A^{\mu}_{\mathrm{G}}(x) = (-\mathbf{F}\cdot\mathbf{r}, -\mathbf{e}_k(\mathbf{F}\cdot\mathbf{r})). \tag{3}$$

The coordinate system is oriented with the electric field $\mathbf{F}$ along the x axis and the magnetic field $\mathbf{B}$ along the y axis, with amplitudes $|\mathbf{F}| = |\mathbf{B}| = F$. The CCF can be considered as the infinite-wavelength limit of a plane wave. In the radiation gauge, it is described by the potential $A^{\mu} = \tilde{a}^{\mu}\varphi_k$, with $\tilde{a}^{\mu} = (0, -a, 0, 0)$, which is linear in the phase $\varphi_k = k\cdot x$. Note that, when performing calculations in a CCF, it proves useful to introduce a wave four-vector $k^{\mu} = \frac{\omega}{c}(1, \mathbf{e}_z)$, along with some frequency ω as an auxiliary quantity. Accordingly, $\mathbf{e}_k = \mathbf{e}_z$ in Eq. (3). Evidently, all observables must be independent of the parameter ω at the end.

The expression (1) would describe the exact transition amplitude if the final state accounted for the interaction of the ionized electron with both the CCF and the nuclear Coulomb field. However, such states are not known in analytical form. In the standard SFA, one disregards the influence of the Coulomb field in the continuum state and approximates the latter by a Volkov wave function, which is an exact solution of the Dirac equation in a plane-wave-like field. In the case of a CCF it reads

$$\psi^{(-)}(x) = \sqrt{\frac{c}{p_0}}\left(1 - \frac{\not{k}\not{A}}{2c(k\cdot p)}\right)u_{p,s}\exp(iS^{(-)}) \times \exp[-i(\tilde{a}\cdot x)\varphi_k/c], \tag{4}$$

with the action

$$S^{(-)} = -(p\cdot x) + \frac{1}{c(k\cdot p)}\left(\frac{(p\cdot\tilde{a})}{2}\varphi_k^2 - \frac{a^2}{6c}\varphi_k^3\right),$$

a free Dirac spinor $u_{p,s}$, and the asymptotic electron momentum $p^{\mu} = (p_0, \mathbf{p})$, where $p_0 = E_p/c$. The second exponential function in (4) stems from the gauge transformation from the radiation to the Göppert-Mayer gauge.

In Eq. (1), following [2,3], the term

$$\left(1 - \frac{\not{A}\not{k}}{2c(k\cdot p)}\right)\exp\left(-i\frac{(p\cdot\tilde{a})}{2c(k\cdot p)}\varphi_k^2 + i\frac{a^2}{6c^2(k\cdot p)}\varphi_k^3 + i\frac{(\tilde{a}\cdot x)}{c}\varphi_k\right) = \int_{-\infty}^{\infty} ds\, e^{-is\varphi_k}\left(\mathcal{A}(s) + i\frac{\not{a}\not{k}}{2c(k\cdot p)}\mathcal{A}'(s)\right) \tag{5}$$

is expressed by a Fourier integral, where

$$\mathcal{A}(s) = \frac{1}{2\pi}\int_{-\infty}^{\infty} d\varphi_k e^{i\varphi_k s}\exp\left(-i\frac{(p\cdot\tilde{a})}{2c(k\cdot p)}\varphi_k^2 + i\frac{a^2}{6c^2(k\cdot p)}\varphi_k^3 + i\frac{(\tilde{a}\cdot x)}{c}\varphi_k\right) \tag{6}$$

and the prime denotes the derivative with respect to s. Now the integration over t in Eq. (1) can be carried out; the resulting $2\pi\delta(E_p - E_{1s} - s\omega)$ is then exploited to perform the integration over s. For the remaining calculations the vector $\mathbf{q} = \mathbf{p} - s\mathbf{k} - \frac{a}{c}\varphi_k\mathbf{e}_x$ and the variables $\alpha = \frac{p\cdot\tilde{a}}{c(k\cdot p)}$, $\beta = \frac{a^2}{8c^2(k\cdot p)}$, and $y = (4\beta)^{2/3}[\frac{s}{4\beta} - (\frac{\alpha}{8\beta})^2]$, with $s = \frac{E_p - E_{1s}}{\omega}$, are introduced and the substitution $z = (4\beta)^{1/3}(\varphi_k - \frac{\alpha}{8\beta})$ is applied, which leads to

$$S^{\mathrm{SFA}} = -\frac{i}{\omega}\sqrt{\frac{c}{p_0}}(4\beta)^{-1/3}\int_{-\infty}^{\infty} dz\int d^3\mathbf{r}\, e^{-i(\mathbf{q}\cdot\mathbf{r})}g(r)\bar{u}_{p,s} \times\left(1 - \frac{\not{a}\not{k}}{2c(k\cdot p)}\varphi_k\right)\not{A}_{\mathrm{G}}\chi_s \times\exp\left[i\left(yz + \frac{z^3}{3}\right)\right]\exp\left[-i\frac{8\beta}{3}\left(\frac{\alpha}{8\beta}\right)^3 + i\frac{\alpha s}{8\beta}\right]. \tag{7}$$

In order to obtain the differential ionization rate, the absolute square of the transition amplitude has to be taken and averaged (summed) over the initial (final) spin polarizations. In carrying out these steps, we use Ref. [4] as orientation (see also [39,40]) but adjust our calculation to the Göppert-Mayer gauge. As a consequence of the latter, the resulting traces over Dirac matrices are simplified decisively, in particular by the fact that the four-products $A_{\mathrm{G}}^2(x) = A_{\mathrm{G}}(x)\cdot A(x) = A_{\mathrm{G}}(x)\cdot k = A(x)\cdot k = k^2 = A_{\mathrm{G}}(x)\cdot A_{\mathrm{G}}(x') = 0$ disappear. The remaining spatial integrations are proportional to

$$|S^{\mathrm{SFA}}|^2 \propto \int d^3\mathbf{r}\int d^3\mathbf{r}' e^{-i(\mathbf{q}\cdot\mathbf{r})}e^{i(\mathbf{q}'\cdot\mathbf{r}')}g(r)g(r') \times(c_0 + c_3)r'\sin\vartheta'\cos\varphi' r\sin\vartheta\cos\varphi, \tag{8}$$

with

$$c_0 = 1 + \tau^2[\cos\vartheta\cos\vartheta' + \sin\vartheta\sin\vartheta'\cos(\varphi - \varphi')], \quad c_3 = i\tau(-\cos\vartheta + \cos\vartheta'), \tag{9}$$

and can be calculated straightforwardly in analogy to [4]. Herein $\mathbf{q}' = \mathbf{p} - s\mathbf{k} - \frac{a}{c}(k\cdot x')\mathbf{e}_x$ and $\tau = (1-\sigma)c/Z$.

The remaining integrations are of the form

$$\int dz\,\frac{(Z - iQ)^\nu \pm (Z + iQ)^\nu}{[f'(z)]^\nu}\exp[-f(z)], \tag{10}$$

with $f(z) = -i(yz + z^3/3)$, and can be solved by the saddle-point method. The physically relevant saddle point is given by $z_0 = i\sqrt{y}$ and the second derivative reads $f''(z) = -2iz$. To this end, the denominator is expanded according to $f'(z) \approx (z - z_0)f''(z_0)$ and the formula [41]

$$\int\frac{\exp[-\lambda f(x)]}{(x - x_0)^\nu}dx \approx i^\nu\frac{\Gamma(\nu/2)}{2\Gamma(\nu)}\left(\frac{2\pi}{\lambda f''(x_0)}\right)^{1/2} \times[2\lambda f''(x_0)]^{\nu/2}\exp[-\lambda f(x_0)] \tag{11}$$

is applied that is valid for large values of λ. To satisfy the conditions for the applicability of (11), the condition $y \gg 1$ must be ensured in Eq. (7).

By using the saddle-point method, the previously purely real quantity $\mathbf{q}$ becomes complex,

$$q_x = -\frac{az}{c(4\beta)^{1/3}} = -i\frac{\varepsilon}{c}, \quad q_\perp = \sqrt{q_x^2 + q_y^2} = i\frac{\zeta}{c}, \quad q = \sqrt{q_x^2 + q_y^2 + q_z^2} = i\frac{\eta}{c},$$

with the abbreviations

$$\gamma = p_0 - p_z, \quad \eta = \sqrt{c^4 - E_{1s}^2}, \quad \varepsilon = \sqrt{\eta^2 + p_y^2c^2 + (c\gamma - E_{1s})^2}, \quad \zeta = \sqrt{\eta^2 + (c\gamma - E_{1s})^2}. \tag{12}$$

The rate is determined by integrating the resulting expression in the common way over the momentum space and by dividing it by the interaction time T,

$$R = \int\frac{d^3\mathbf{p}}{(2\pi)^3}\frac{|S^{\mathrm{SFA}}|^2}{T}. \tag{13}$$

Noticing that $|S^{\mathrm{SFA}}|^2$ does not depend on p_x, the corresponding integral in Eq. (13) yields

$$\int dp_x = FT \tag{14}$$

(see also [2,42]). The remaining p_y and p_z integrations are transformed into integrations over p_y and γ, according to

$$R = \frac{F^2C_{1s}^2}{4}(2Z)^{2\sigma-2}\int_{-\infty}^{\infty}dp_y\int_0^\infty d\gamma\,\frac{\gamma}{\varepsilon}e^{-(4/3)y^{3/2}}\{|\tilde{S}_1(p_y,\gamma)|^2 + \tau^2[|\tilde{S}_2(p_y,\gamma)|^2 + |\tilde{S}_3(p_y,\gamma)|^2 + |\tilde{S}_4(p_y,\gamma)|^2] + 2\tau\,\mathrm{Re}[\tilde{S}_1(p_y,\gamma)]\mathrm{Im}[\tilde{S}_2(p_y,\gamma)]\}, \tag{15}$$

where

$$\tilde{S}_1(p_y,\gamma) = \varepsilon\left[\frac{c^2}{\eta^3}\Gamma\left(\frac{\sigma+1}{2}\right)D^{\sigma+1} - \frac{c}{\eta^2}\Gamma\left(\frac{\sigma+2}{2}\right)D^{\sigma+2}\right],$$

$$\tilde{S}_2(p_y,\gamma) = i\varepsilon\,q_z\left[3\frac{c^4}{\eta^5}\Gamma\left(\frac{\sigma}{2}\right)D^\sigma - 3\frac{c^3}{\eta^4}\Gamma\left(\frac{\sigma+1}{2}\right)D^{\sigma+1} + \frac{c^2}{\eta^3}\Gamma\left(\frac{\sigma+2}{2}\right)D^{\sigma+2}\right],$$

$$\tilde{S}_3(p_y,\gamma) = -\frac{\varepsilon}{\zeta}\left[\left(3\frac{\zeta^2c^3}{\eta^5}-\frac{c^3}{\eta^3}\right)\Gamma\left(\frac{\sigma}{2}\right)D^\sigma + \left(\frac{c^2}{\eta^2}-3\frac{\zeta^2c^2}{\eta^4}\right)\Gamma\left(\frac{\sigma+1}{2}\right)D^{\sigma+1} + \frac{\zeta^2c}{\eta^3}\Gamma\left(\frac{\sigma+2}{2}\right)D^{\sigma+2}\right],$$

$$\tilde{S}_4(p_y,\gamma) = -i\frac{p_yc}{\zeta}\left[\frac{c^3}{\eta^3}\Gamma\left(\frac{\sigma}{2}\right)D^\sigma - \frac{c^2}{\eta^2}\Gamma\left(\frac{\sigma+1}{2}\right)A^{\sigma+1}\right],$$

with $D = Zc(\frac{2}{F\gamma\varepsilon})^{1/2}$.

The remaining integrations can be carried out by numerical means without difficulties.

B. Coulomb correction

Up to this point, the influence of the Coulomb field on the continuum state has not been considered. However, especially during the tunneling process, the electron continues to experience the influence of this field. Therefore, what is needed is a way to account for the effect of the nucleus on the ionized electron. For an electron bound by a short-range potential, this problem has already been widely treated [7–9,19–21]. Accordingly, to include the Coulomb interaction between the atomic core and the escaping electron in this case, its influence is taken into account under the complete tunneling barrier. This is achieved by dividing the barrier length into rather close distances, where the Coulomb effects can be incorporated via a typical Coulomb logarithm in the wave function, and rather large distances, where the Coulomb potential can be treated as a perturbation, with both regions being linked through a matching procedure [7–9,19–21].

In our case, however, we do not assume short-range binding forces but instead fully account for the long-range nuclear Coulomb field in the bound $1s$ state. A part of the total Coulomb effects is therefore already contained in Eq. (15). As a consequence, we have to appropriately truncate the Coulomb corrections established in [7–9,19–21] in order to avoid their overestimation. To this end, we restrict the influence on the escaping electron to the region in which the Coulomb field, as compared with the impact of the CCF, is a perturbation. It will turn out that this procedure provides a remarkably good approximation to the Coulomb effects.

We determine the Coulomb correction as [7–9,19–21]

$$Q = \exp\left(2iZ\int_{t_1}^{0}\frac{1}{r(t)}dt\right), \tag{16}$$

where $t = t_1$ denotes the time at which the Coulomb potential starts to be taken into account and $t = 0$ denotes the time of the tunnel exit.

The trajectory $r(t)$ is obtained by a solution of the classical relativistic equations of motion in a CCF, which is adapted to the initial conditions $\vec{r}(t_0) = 0$, $\mathrm{Im}[\vec{r}(0)] = 0$, $\mathrm{Im}[\dot{\vec{r}}(0)] = 0$, and $\frac{1}{\sqrt{1-\dot{\vec{r}}^2(t_0)/c^2}} = \epsilon_0$, with $\epsilon_0 = E_{1s}/c^2$. Here $t(u_0) = t_0$ is the time of tunnel entry. This results in the parametrized coordinates [7,20,21]

$$x(u) = \frac{c^2}{2F\lambda}\left(u^2-u_0^2\right),\quad y(u)=0,\quad z(u) = i\frac{c^2}{6F\lambda}\left(u_0^2-u^2\right)u,$$

$$ct(u) = i\frac{c^2}{2F\lambda}(1+\lambda^2)u - i\frac{c^2}{6F\lambda}u^3, \tag{17}$$

with $u_0^2 = 3(\lambda^2-1)$ and $\lambda = -\frac{\epsilon_0}{2} + \frac{1}{2}\sqrt{\epsilon_0^2+8}$.

An intuitive approach to determine t_1 is motivated by the idea that for $r_1 = r(t_1)$ the Coulomb field strength equals the CCF amplitude and afterward falls below it. This leads to

$$r_1 = \sqrt{\frac{Z}{F}}. \tag{18}$$

We note that r_1, while being substantially larger than the size of approximately $1/Z$ of the bound state, is much smaller than the extension of approximately Z^2/F of the tunneling barrier. From this, also u_1 can be determined:

$$\frac{c^2}{2F\lambda}\left(u_0^2-u^2\right)\sqrt{1-\frac{u^2}{9}} = r_1. \tag{19}$$

Taking the tunnel distance as a pure x component, where $|x(u)| \gg |z(u)|$ holds, the equation is simplified to

$$u_1 = \sqrt{u_0^2 - \frac{2F^{1/2}Z^{1/2}\lambda}{c^2}}. \tag{20}$$

Interestingly, the intuitive value of r_1 (as well as the associated coordinate x_1) given above can be mathematically supported and further improved by noting that it coincides approximately with the saddle point of the integrand in the S-matrix element of Eq. (1). Let us briefly sketch the corresponding derivation [43]. The space-time dependence of the integrand in cylindrical coordinates is given by

$$m = \rho^2\cos(\phi)e^{-iS[\rho,\phi,z,t]}(2Z\sqrt{\rho^2+z^2})^{\sigma-1}e^{-Z\sqrt{\rho^2+z^2}}e^{-i\sigma c^2t}, \tag{21}$$

where $S[\rho,\phi,z,t]$ denotes the classical action, which satisfies the Hamilton-Jacobi equation

$$\left(\nabla S + \frac{1}{c}\mathbf{A}_\mathrm{G}\right)^2 - \frac{1}{c^2}\left(\frac{\partial S}{\partial t} - A_\mathrm{G}^0 - \frac{Z}{r}\right)^2 + c^2 = 0. \tag{22}$$

Note that the angular dependence of the spinors $\chi_{\pm\,1/2}$ has been omitted in Eq. (21), as it is contained solely in the lower components which are suppressed by the small parameter τ. We can now substitute the saddle-point conditions into this equation and obtain an equation for x, which can be solved approximately by exploiting the smallness of F/F_a (with the atomic field strength $F_a = Z^3$) and I_p/c^2. With next-to-leading order accuracy, we find

$$\tilde{x}_1 = -\sqrt{\frac{Z}{F}}\left(1+\frac{Z^2}{9c^2}\right) + \frac{1}{Z} \tag{23}$$

and

$$\tilde{u}_1 = \sqrt{u_0^2 + \frac{2F\lambda}{c^2}\tilde{x}_1}. \tag{24}$$

We point out that here we have taken the influence of the z component into account, which modifies the second term in

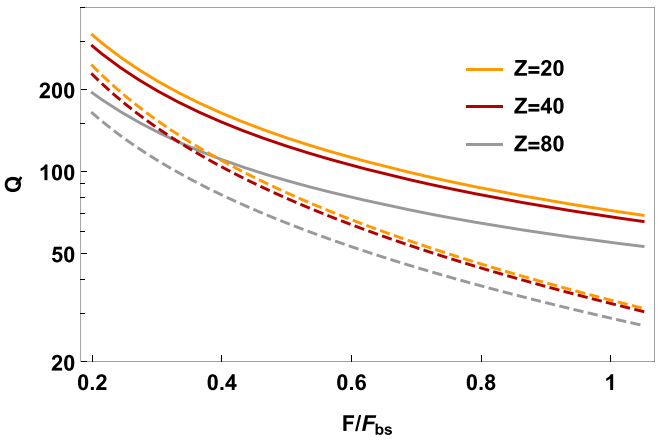

FIG. 1. Coulomb-correction factor from Eq. (25) as a function of the normalized field strength F/F_{bs}, where $F_{bs} = c^4(1-\sigma)^2/4Z$ denotes the barrier suppression field strength. For comparison, the Coulomb-correction factor for the intuitive approach with $\varphi_1 = \arcsin(u_1/3)$ [see Eq. (20)] is shown as dashed curves.

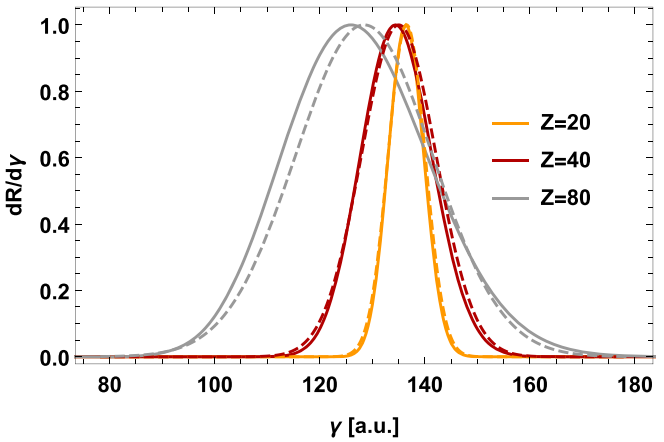

FIG. 2. Differential rate $\frac{dR}{d\gamma}$ as a function of γ for different nuclear charge numbers Z at $F = F_{bs}$ (solid lines), when the p_y dependence in Eq. (15) has been integrated numerically. The dashed lines show the approximation when the exponential prefactor in Eq. (15) is evaluated at $p_y = 0$ and $\gamma = \gamma_0$, the p_y dependence is integrated out analytically, and the remaining exponent is expanded up to second order. The curves have been normalized to a height of 1 to facilitate their comparison.

parentheses in Eq. (23). The Coulomb correction is accordingly determined to

$$Q = \left(\frac{\sin(\varphi_0+\varphi_1)}{\sin(\varphi_0-\varphi_1)}\right)^{2\delta} \exp\left(\frac{6Z\varphi_1}{c}\right), \tag{25}$$

where $\delta = Z\epsilon_0(1-\epsilon_0^2)^{-1/2}/c$, $\varphi_0 = \arcsin(u_0/3)$, and $\varphi_1 = \arcsin(\tilde{u}_1/3)$.

For illustration, Fig. 1 shows the Coulomb-correction factor from Eq. (25) by solid lines and the intuitive correction factor based on Eq. (20) by dashed lines. The more accurate description yields larger corrections, especially at high field strength. Compared to the well-known result of [7], however, the present Coulomb-correction factors turn out to be much smaller (by about two orders of magnitude). As mentioned before, this is because in [7] the correction is evaluated along the complete tunnel length.

Before moving on to the next section, we note that a general criterion for applicability of the Coulomb-factor approximation in SFA calculations has been established in [44]. Since the Coulomb correction is obtained via semiclassical electron trajectories, artifacts in the form of artificial Coulomb singularities can in principle arise when the electron comes too close to the nucleus. This may happen, for example, due to recollisions in linearly polarized laser fields in a nonrelativistic interaction regime when the dipole approximation applies. In our case of a CCF, however, the electron always remains far from the core and never returns: Already at the saddle point, from where we start to account for the Coulomb correction, we have $r_1/r_a \approx \sqrt{F_a/F} \gg 1$ (with the atomic Bohr radius $r_a \approx 1/Z$) and the electron-core distance continues to grow for later times. Recollisions are generally suppressed by a magnetic-field component due to the magnetic part of the Lorentz force that induces a drift motion of the electron (see, e.g., [11]). The applicability condition for a Coulomb-correction factor from Ref. [44] is therefore fulfilled.

C. Analytical simplifications

The fact that the prefactor of the exponential dependence $e^{-(4/3)y^{3/2}}$ in Eq. (15) changes only very slowly as a function of γ and p_y can now be used to solve the remaining integrations. The p_y dependence is contained in the variables ε and ζ, as well as in the exponential dependence by the variable y. In order to be able to carry out the integration over p_y, the prefactor is evaluated at $p_y = 0$ and the function in the exponential is expanded around $p_y = 0$ up to the second order. The p_y dependence in Eq. (15) can then be evaluated analytically as a Gaussian integral to a very good approximation.

The γ dependence is far more complex. Nevertheless, it proves to be practicable to integrate only over the exponential dependence. Therefore, the value γ_0 is determined at which the exponential function reaches its maximum:

$$\gamma_0 = \frac{E_{1s}}{4c} + \frac{1}{4c}\sqrt{E_{1s}^2 + 8c^4}. \tag{26}$$

The exponent is expanded up to the second order around γ_0 and the prefactor is evaluated at this point. That this approach reflects the differential rate from Eq. (15) very well can be seen in Fig. 2. Here $dR/d\gamma$ from Eq. (15) is shown as a solid line for different nuclear charge numbers Z. In comparison, the approach described above by evaluating the prefactor at γ_0 and expanding the exponent is shown as a dashed line. The maximum of the exact differential rate lies only slightly below γ_0 and the widths of both curves (for given Z) are almost the same [45]. By formally extending the lower integration boundary to $-\infty$, the γ integration over the approximated expression for $dR/d\gamma$ can be performed as a Gaussian integral as well. This results in

$$R = \frac{1}{4}\pi F^2 C_{1s}^2 (2Z)^{2\sigma-2}\frac{\gamma_0}{\varepsilon_0}\sqrt{\frac{2F\gamma_0}{\varepsilon_0 h''(\gamma_0)}}\, e^{-h(\gamma_0)} \times \{|\tilde{S}_1(p_y=0,\gamma=\gamma_0)|^2$$

$$+\tau^2[|\tilde{S}_2(p_y=0,\gamma=\gamma_0)|^2+|\tilde{S}_3(p_y=0,\gamma=\gamma_0)|^2]$$
$$+2\tau\,\mathrm{Re}[\tilde{S}_1(p_y=0,\gamma=\gamma_0)]\mathrm{Im}[\tilde{S}_2(p_y=0,\gamma=\gamma_0)]\},\tag{27}$$

where

$$\varepsilon_0=\sqrt{\eta^2+(c\gamma_0-E_{1s})^2},$$
$$h(\gamma)=\frac{2\varepsilon^3}{3c^2F\gamma}.$$

To further simplify the expression, γ_0 can be expanded for small values of $I_p/c^2\ll 1$ to give

$$\gamma_0\approx c-\frac{I_p}{3c}.\tag{28}$$

Accordingly, the main contribution of p_z is around $\frac{I_p}{3c}$. This behavior is in agreement with the result of [26], where the same shift of the momentum distribution along this direction has been found. It originates from the influence of the magnetic-field component that causes, in classical terms, a $-\frac{1}{c}\mathbf{v}\times\mathbf{B}$ force in addition to the electric-field force. As long as the electron velocity $\mathbf{v}$ is much smaller than c, the electric-field force is dominant, so $\mathbf{v}$ is mainly oriented along the negative x direction in our frame of coordinates. The magnetic field $\mathbf{B}$ along y thus leads to a Lorentz force on the electron that points in the positive z direction and this way causes the characteristic shift in the p_z distribution. For ionization in a purely electric field such a shift is accordingly absent [21,26,38].

By noting that the magnetic-field-induced shift Δp_z emerges during the subbarrier motion of the electron [26,38] and that the tunneling time amounts to $\tau_t\sim Z/F$ [1,21], the shift can be roughly estimated by order of magnitude as $\Delta p_z\sim\frac{v}{c}F\tau_t\sim I_p/c$, with the atomic velocity $v\sim Z$ of the electron. This physically intuitive argument can, in particular, explain why the value of the magnetic-field-induced momentum shift is independent of the field amplitude F.

The shift is especially important for highly charged ions where I_p is large. More precisely, the shift becomes particularly distinct when it is comparable to or even larger than the width of approximately $\sqrt{F/Z}$ of the p_z momentum distribution, that is, when $Z/c\gtrsim\sqrt{F/F_a}$ holds.

By noticing in Eq. (27) that $|\tilde{S}_1|\gg\tau|\tilde{S}_i|$ for $i\in\{2,3,4\}$ holds in the relevant range of parameters, especially for small and medium-sized Z, and by expanding all quantities up to the first order in $I_p/c^2\ll 1$, the rate can be approximately written as

$$R\approx\frac{F^{2-\sigma}F_a^{1+4\sigma/3}}{(2I_p)^{7/2+\sigma/2}}\frac{1+\sigma}{\Gamma(1+2\sigma)}2^{3\sigma-3}\frac{1-\frac{7}{72}\frac{I_p}{c^2}}{\sqrt{1+\frac{5}{12}\frac{I_p}{c^2}}}$$
$$\times\frac{1}{(1-\frac{1}{2}\frac{I_p}{c^2})^3}\Gamma\left(\frac{\sigma+1}{2}\right)^2\left(1+\frac{17}{36}\frac{I_p}{c^2}\right)^{\sigma}$$
$$\times\left\{1-\frac{\Gamma\left(\frac{\sigma+2}{2}\right)}{\Gamma\left(\frac{\sigma+1}{2}\right)}Z\left[2\frac{\sqrt{2I_p}}{F}\left(1-\frac{1}{36}\frac{I_p}{c^2}\right)\right]^{1/2}\right\}^2$$
$$\times\exp\left[-\frac{2}{3}\frac{(2I_p)^{3/2}}{F}\left(1-\frac{1}{12}\frac{I_p}{c^2}\right)\right],\tag{29}$$

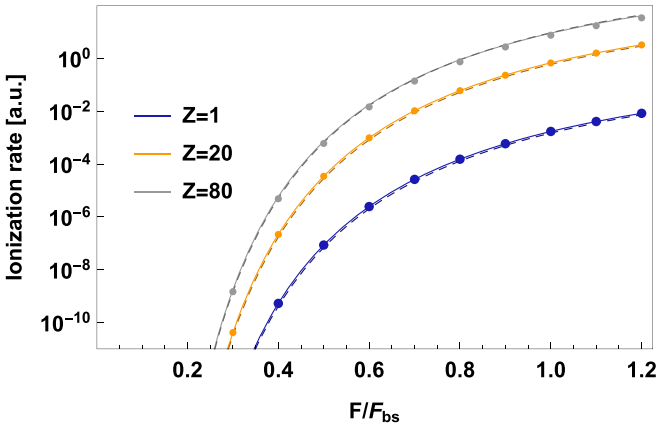

FIG. 3. Total ionization rate as a function of the normalized field strength F/F_{bs}. The solid curves show Eq. (27) corrected by the Coulomb factor (25), the corresponding analytical approximation (29) including the same Coulomb factor is depicted by circles, and the Coulomb-corrected rate of [20,21] is shown as dashed curves.

with the atomic field strength $F_a=Z^3$. While the exponential characteristic of the ionization process $\exp[-\frac{2}{3}\frac{(2I_p)^{3/2}}{F}]$ is generally found in tunnelinglike rate expressions [1–3,7–9,19–21], it is particularly noteworthy that the additional term $I_p/12c^2$ in the last line of Eq. (29) coincides as well with that of Ref. [26]. The various relativistic ionization theories are known to somewhat differ in the nuclear charge and field strength dependences of the preexponential factors they predict.

To account for the Coulomb correction, the standard SFA rate from Eq. (15) as well as (27) has to be multiplied by the factor Q:

$$R_Q=R\cdot Q.\tag{30}$$

In the next section the rate R_Q is compared with previously existing calculations and it is placed in context.

III. RESULTS AND DISCUSSION

In this section we illustrate our theoretical approach by showing the resulting ionization rates in a wide range of field strengths and ionic systems. Moreover, we compare our findings with already existing calculations of relativistic strong-field ionization.

The dependence on the field strength is mainly determined by the exponential dependence of the rate. Different ionization theories can, however, differ in the preexponential factors they predict.

Figure 3 shows the total ionization rate (27) corrected by the Coulomb factor (25) as a function of the normalized field strength (solid curves). The steep exponential dependence is clearly seen. For comparison, the PPT result of [20,21] is presented as dashed curves. On the displayed logarithmic scale, our results lie almost completely on the PPT curves and differ only slightly.

The dotted curves give the Coulomb-corrected equation (29). The approximation coincides very well with the solid curves and deviates only slightly from this result for large nuclear charge numbers Z and large field strengths. The

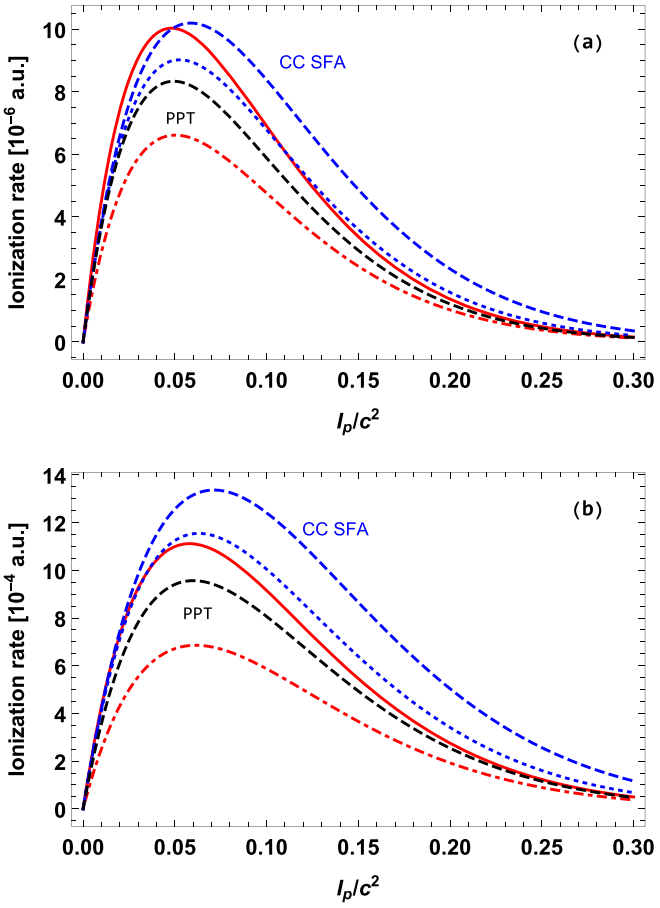

FIG. 4. Total ionization rate as a function of the normalized ionization potential I_p/c^2 for (a) $F/F_a = \frac{1}{32}$ and (b) $F/F_a = \frac{1}{25}$. The red solid lines show the (over half a cycle of an oscillating laser wave averaged) results from Eq. (27), including the Coulomb-correction factor (25). The red dot-dashed lines show the result for the intuitive Coulomb-correction factor with $\varphi_1 = \arcsin(u_1/3)$ [see Eq. (20)]. The blue dashed (dotted) curves represent Eq. (78) [Eq. (97)] from [26] and the black dashed lines shows the cycle-averaged result of [20,21].

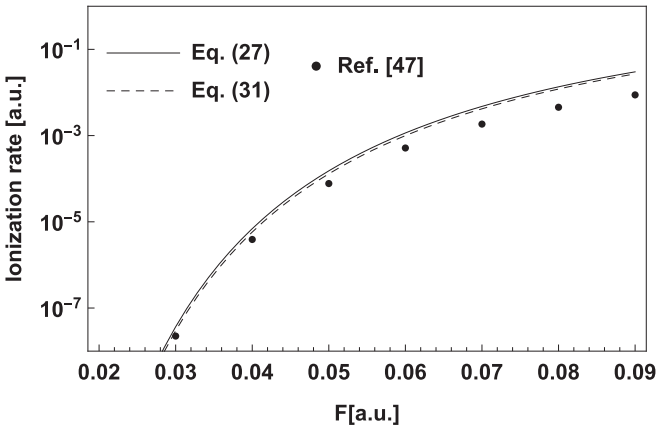

FIG. 5. Total ionization rates of a hydrogen atom, depending on the applied field strength. The solid curve shows the relativistic rate in the CCF [our Eq. (27) with Coulomb correction], the dashed curve the nonrelativistic rate in the SEF [Eq. (31)], and the circles the relativistic rates in the SEF from [48]. The barrier-suppression field is $F_{bs}(Z = 1) \approx 0.06$ a.u. here.

dependence of the ionization rate on the nuclear charge, which is encoded by the normalized ionization potential, is shown in Fig. 4 on a linear scale. Our rate in a CCF has been averaged over half a cycle of an oscillating laser wave with an electric field of the form $F \sin(\varphi_k)$. It is compared with the PPT results from Refs. [20,21] (also averaged over half a laser period) and the SFA results from Ref. [26], where ionization by a linearly polarized laser wave was considered. We note in this regard that Eqs. (78) and (97) in Ref. [26] represent two variants of the Coulomb-corrected SFA that are obtained from different partitions of the underlying Hamiltonian. While Eq. (78) relies on the standard partition, in the dressed Coulomb-corrected SFA of Eq. (97) the laser field makes some contribution to the bound-state evolution. The latter brings the rates closer to the PPT prediction. When we apply our intuitive Coulomb-correction factor based on Eq. (20), the ionization rate comes out a bit too low, as the red dashed curves show. This correction factor thus slightly underestimates the Coulomb effects. The shape of the curves is however very similar to the PPT result of [20,21] and Eq. (97) from [26]. Applying the more accurate Coulomb correction (25) improves the ionization rates significantly (red solid curves). Now they resemble more closely the predictions from [26] that include the Coulomb effects in a coherent manner by using eikonal Volkov states. The remaining differences as compared with this advanced SFA theory indicate that further correction terms (especially those stemming from the innermost region of the tunnel) would be needed in our approach to enhance the agreement.

To conclude this section, we discuss the relation of our results in a CCF with ionization rates in a static electric field (SEF). While a magnetic-field component plays an important role for the momentum distributions of emitted photoelectrons (see [21,26] and Sec. II C), it has been shown in [21] that the total relativistic ionization rates in the CCF and SEF are almost identical. Especially in the nonrelativistic regime of laser-atom interaction, the magnetic-field component can usually be neglected and the dipole approximation applied. The nonrelativistic rate for tunneling ionization in an SEF is given by the well-known formula [46]

$$R_{\mathrm{SEF}}^{(\mathrm{nr})} = \frac{4Z^5}{F} \exp\left(-\frac{2Z^3}{3F}\right). \tag{31}$$

Figure 5 shows a comparison of this formula with the prediction from our approach [Eq. (27) including the Coulomb correction (25)]. Both curves run nearly parallel, with our results overestimating the rate (31) slightly: by about 23% at $F = 0.03$ a.u. and continuously decreasing to about 11% at $F = 0.09$ a.u. The deviations are caused by the approximations made in our treatment. We note that the relativistic ionization rate in an SEF from [21], which is obtained from a quasiclassical approach, would practically coincide with the nonrelativistic rate (31) in the considered range of field strengths. Total rates for relativistic ionization have also been calculated numerically by the method of complex scaling utilizing a finite-basis expansion [47,48]. The corresponding results are included in Fig. 5 as circles. For small field

strengths $F \approx 0.03$ a.u., all approaches yield very similar ionization rates. For larger fields, however, the complex-scaling method provides smaller rates, indicating that the tunneling theories lead to overestimations when approaching or even exceeding the over-barrier threshold. This conclusion is in accordance with corresponding results obtained from fully numerical solutions of the Schrödinger equation [49].

While Fig. 5 refers to a nonrelativistic system with $Z = 1$, we emphasize that relativistic effects can become very significant in highly charged ions. In order to quantify them we compare our Coulomb-corrected equation (27) with the predictions from Eq. (31). For example, at $F = 0.1F_{bs}$ ($F = 0.3F_{bs}$) the relativistic-to-nonrelativistic ratio of total rates amounts to approximately 0.6 (approximately 0.94) for $Z = 20$ to approximately 0.048 (approximately 0.37) for $Z = 40$ and to approximately 1.5×10^{-6} (approximately 7.4×10^{-3}) for $Z = 80$. At large values of Z, our treatment thus predicts a very substantial reduction of the ionization rate due to relativistic effects, in accordance with the results of Ref. [21]. We note that this general trend is in correspondence with the increase of the binding potential I_p due to relativistic effects, which makes it harder to ionize the bound electron than one would expect on the basis of a nonrelativistic description.

IV. CONCLUSION

An alternative treatment of relativistic strong-field ionization of hydrogenlike atomic systems has been presented. Our approach combines various calculational methods that have been developed in earlier investigations of the problem [2–4,7]. First, we calculated the total ionization rate of a $1s$ electron bound by a nuclear Coulomb potential in the presence of a constant crossed field in the Göppert-Mayer gauge within Dirac theory and standard SFA. To take the influence of the Coulomb field on the electron continuum state during tunneling into consideration, a well-known method that relies on the assumption of a short-range binding potential [7] was adjusted appropriately. Two versions of the resulting modified Coulomb-correction factor were obtained, an intuitive one and a more accurate one, that are effectively active in the region where the nuclear Coulomb field has fallen below the CCF. They may be interpreted as arising from the necessity to incorporate Coulomb effects into the Volkov state. We emphasize that both versions of our Coulomb-correction factor represent approximations as they disregard the innermost subbarrier region.

We have derived a representation of the Coulomb-corrected total ionization rate as a double integral, which could be very well approximated by an analytical formula in closed form. Comparing our corresponding results with predictions from previous studies based on PPT [20,21] or Coulomb-corrected SFA [26] theories, we found good agreement in a wide range of nuclear charges (ionization potentials) for field strengths below the barrier suppression field. Our study may offer additional insights into relativistic strong-field ionization, in general, and the role of Coulomb corrections, in particular. It may, moreover, help to establish further connections between corresponding PPT and SFA theories.

As an outlook we note that our approach could be appropriately applied to other strong-field problems as well to obtain, for example, a Coulomb-corrected rate for bound-free pair production in an intense laser field [39,40].

ACKNOWLEDGMENTS

This work was funded by the Deutsche Forschungsgemeinschaft under Grant No. 392856280 within the Research Unit FOR 2783/1. Useful discussions with K. Z. Hatsagortsyan are gratefully acknowledged.

[1] L. V. Keldysh, Ionization in the field of a strong electromagnetic wave, Zh. Eksp. Teor. Fiz. **47**, 1945 (1964) [Sov. Phys. JETP **20**, 5 (1965)].

[2] A. I. Nikishov and V. I. Ritus, Ionization of systems bound by short-range forces by the field of an electromagnetic wave, Zh. Eksp. Teor. Fiz. **50**, 255 (1966) [Sov. Phys. JETP **23**, 168 (1966)].

[3] A. I. Nikishov and V. I. Ritus, Ionization of atoms by an electromagnetic-wave field, Zh. Eksp. Teor. Fiz. **52**, 223 (1967) [Sov. Phys. JETP **25**, 145 (1967)].

[4] H. R. Reiss, Relativistic strong-field photoionization, J. Opt. Soc. Am. B **7**, 574 (1990).

[5] H. R. Reiss, Complete Keldysh theory and its limiting cases, Phys. Rev. A **42**, 1476 (1990).

[6] A. M. Perelomov and V. S. Popov, Ionization of atoms in an alternating electrical field III, Zh. Eksp. Teor. Fiz. **52**, 514 (1967) [Sov. Phys. JETP **25**, 336 (1967)].

[7] V. D. Mur, B. M. Karnakov, and V. S. Popov, Relativistic version of the imaginary-time formalism, Zh. Eksp. Teor. Fiz. **114**, 798 (1998) [Sov. Phys. JETP **87**, 433 (1998)].

[8] V. S. Popov, B. M. Karnakov, and V. D. Mur, Relativistic version of the imaginary-time method, Phys. Lett. A **250**, 20 (1998).

[9] V. S. Popov, B. M. Karnakov, V. D. Mur, and S. G. Pozdnyakov, Relativistic theory of tunnel and multiphoton ionization of atoms in a strong laser field, JETP **102**, 760 (2006).

[10] H. R. Reiss, Theoretical methods in quantum optics: S-matrix and Keldysh techniques for strong-field processes, Prog. Quantum Electron. **16**, 1 (1992).

[11] A. Di Piazza, C. Müller, K. Z. Hatsagortsyan, and C. H. Keitel, Extremely high-intensity laser interactions with fundamental quantum systems, Rev. Mod. Phys. **84**, 1177 (2012).

[12] K. Krajewska, F. Cajiao Vélez, and J. Z. Kamiński, *Advances in Optics* (IFSA, Barcelona, 2018), Vol. 2, pp. 145–176.

[13] C. I. Moore, A. Ting, S. J. McNaught, J. Qiu, H. R. Burris, and P. Sprangle, A Laser-Accelerator Injector Based on Laser Ionization and Ponderomotive Acceleration of Electrons, Phys. Rev. Lett. **82**, 1688 (1999).

[14] K. Yamakawa, Y. Akahane, Y. Fukuda, M. Aoyama, N. Inoue, and H. Ueda, Ionization of many-electron atoms by ultrafast laser pulses with peak intensities greater than 10^{19} W/cm^2, Phys. Rev. A **68**, 065403 (2003).

[15] A. D. DiChiara, I. Ghebregziabher, R. Sauer, J. Waesche, S. Palaniyappan, B. L. Wen, and B. C. Walker, Relativistic MeV Photoelectrons from the Single Atom Response of Argon to a 10^{19} W/cm^2 Laser Field, Phys. Rev. Lett. **101**, 173002 (2008).

[16] A. D. DiChiara, I. Ghebregziabher, J. M. Waesche, T. Stanev, N. Ekanayake, L. R. Barclay, S. J. Wells, A. Watts, M. Videtto, C. A. Mancuso, and B. C. Walker, Photoionization by an ultraintense laser field: Response of atomic xenon, Phys. Rev. A **81**, 043417 (2010).

[17] C. J. Joachain and N. J. Kylstra, Relativistic effects in the multiphoton ionization of hydrogenlike ions by ultrashort infrared laser pulses, Phys. Rev. A **100**, 013417 (2019).

[18] K. Krajewska and J. Z. Kamiński, Supercontinuum in ionization by relativistically intense and short laser pulses: Ionization without interference and its time analysis, Phys. Rev. A **94**, 013402 (2016).

[19] V. S. Popov, Imaginary-time method in quantum mechanics and field theory, Phys. At. Nucl. **68**, 686 (2005).

[20] N. Milosevic, V. P. Krainov, and T. Brabec, Semiclassical Dirac Theory of Tunnel Ionization, Phys. Rev. Lett. **89**, 193001 (2002).

[21] N. Milosevic, V. P. Krainov, and T. Brabec, Relativistic theory of tunnel ionization J. Phys. B **35**, 3515 (2002).

[22] M. Jain and N. Tzoar, Compton scattering in the presence of coherent electromagnetic radiation, Phys. Rev. A **18**, 538 (1978).

[23] S. V. Popruzhenko, V. D. Mur, V. S. Popov, and D. Bauer, Strong Field Ionization Rate for Arbitrary Laser Frequencies, Phys. Rev. Lett. **101**, 193003 (2008).

[24] S. V. Popruzhenko and D. Bauer, Strong field approximation for systems with Coulomb interaction, J. Mod. Opt. **55**, 2573 (2008).

[25] F. Cajiao Vélez, K. Krajewska, and J. Z. Kamiński, Generalized eikonal approximation for strong-field ionization, Phys. Rev. A **91**, 053417 (2015).

[26] M. Klaiber, E. Yakaboylu, and K. Z. Hatsagortsyan, Above-threshold ionization with highly charged ions in superstrong laser fields: II. Relativistic Coulomb-corrected strong-field approximation, Phys. Rev. A **87**, 023418 (2013).

[27] L. Torlina and O. Smirnova, Time-dependent analytical *R*-matrix approach for strong-field dynamics. I. One-electron systems, Phys. Rev. A **86**, 043408 (2012).

[28] L. Torlina, J. Kaushal, and O. Smirnova, Time-resolving electron-core dynamics during strong-field ionization in circularly polarized fields, Phys. Rev. A **88**, 053403 (2013).

[29] S. X. Hu and C. H. Keitel, Dynamics of multiply charged ions in intense laser fields, Phys. Rev. A **63**, 053402 (2001).

[30] S. X. Hu and C. H. Keitel, Spin Signatures in Intense Laser-Ion Interaction, Phys. Rev. Lett. **83**, 4709 (1999).

[31] C. H. Keitel and S. X. Hu, Coherent x-ray pulse generation in the sub-Ångström regime, Appl. Phys. Lett. **80**, 541 (2002).

[32] G. Mocken and C. H. Keitel, FFT-split-operator code for solving the Dirac equation in 2+1 dimensions, Comput. Phys. Commun. **178**, 868 (2008).

[33] H. Bauke, H. G. Hetzheim, G. R. Mocken, M. Ruf, and C. H. Keitel, Relativistic ionization characteristics of laser-driven hydrogenlike ions, Phys. Rev. A **83**, 063414 (2011).

[34] S. Selstø, E. Lindroth, and J. Bengtsson, Solution of the Dirac equation for hydrogenlike systems exposed to intense electromagnetic pulses, Phys. Rev. A **79**, 043418 (2009).

[35] Y. V. Vanne and A. Saenz, Solution of the time-dependent Dirac equation for multiphoton ionization of highly charged hydrogenlike ions, Phys. Rev. A **85**, 033411 (2012).

[36] I. V. Ivanova, V. M. Shabaev, D. A. Telnov, and A. Saenz, Scaling relations of the time-dependent Dirac equation describing multiphoton ionization of hydrogenlike ions, Phys. Rev. A **98**, 063402 (2018).

[37] D. Bauer, D. B. Milosevic, and W. Becker, Strong-field approximation for intense-laser atom processes: The choice of gauge, Phys. Rev. A **72**, 023415 (2005).

[38] M. Klaiber, E. Yakaboylu, H. Bauke, K. Z. Hatsagortsyan, and C. H. Keitel, Under-the-Barrier Dynamics in Laser-Induced Relativistic Tunneling, Phys. Rev. Lett. **110**, 153004 (2013).

[39] C. Müller, A. B. Voitkiv, and N. Grün, Nonlinear Bound-Free Pair Creation in the Strong Electromagnetic Fields of a Heavy Nucleus and an Intense X-Ray Laser, Phys. Rev. Lett. **91**, 223601 (2003).

[40] C. Müller, A. B. Voitkiv, and N. Grün, Few-photon electron-positron pair creation in the collision of a relativistic nucleus and an intense x-ray laser beam, Phys. Rev. A **70**, 023412 (2004).

[41] G. F. Gribakin and M. Y. Kuchiev, Multiphoton detachment of electrons from negative ions, Phys. Rev. A **55**, 3760 (1997).

[42] N. B. Narozhnyi and A. I. Nikishov, Electron-positron pair production by a Coulomb center located in a constant field, Zh. Eksp. Teor. Fiz. **63**, 1135 (1972) [Sov. Phys. JETP **36**, 598 (1973)].

[43] The same kind of method has been used in the nonrelativistic regime of strong-field ionization to describe nonadiabatic effects in the tunneling dynamics; see M. Klaiber, K. Z. Hatsagortsyan, and C. H. Keitel, Tunneling Dynamics in Multiphoton Ionization and Attoclock Calibration, Phys. Rev. Lett. **114**, 083001 (2015).

[44] J. Z. Kaminski, F. Cajiao Velez, and K. Krajewska, Coulomb-corrected strong field approximation without singularities and branching points, J. Phys.: Conf. Ser. **1206**, 012004 (2019).

[45] While the curve heights in Fig. 2 have been normalized, we note that the maxima of the exact numerical evaluation in absolute numbers lie slightly above the analytical approximation by about $3-4\%$ for $F = F_{bs}$ and by less than 1% for $F = 0.1F_{bs}$.

[46] L. D. Landau and E. M. Lifshitz, *Quantum Mechanics* (Pergamon, Oxford, 1965).

[47] I. A. Ivanov and Y. K. Ho, Complex rotation method for the Dirac Hamiltonian, Phys. Rev. A **69**, 023407 (2004).

[48] I. A. Maltsev, D. A. Tumako, R. V. Popov, and V. M. Shabaev, Calculations of relativistic Stark energies and widths in hydrogen-like ions using the complex-scaling method, Opt. Spectrosc. **130**, 455 (2022).

[49] A. Scrinzi, M. Geissler, and T. Brabec, Ionization Above the Coulomb Barrier, Phys. Rev. Lett. **83**, 706 (1999).